Tissue-based metabolic labeling of polysialic acids in living primary hippocampal neurons

Kyungtae Kang[a,b,c,1], Sunghoon Joo[d,1], Ji Yu Choi[a,b,c,1], Sujeong Geum[b,c], Seok-Pyo Hong[a,b,c], Seung-Yeul Lee[e,f], Yong Ho Kim[f], Seong-Min Kim[g], Myung-Han Yoon[g], Yoonkey Nam[d,2], Kyung-Bok Lee[e,2], Hee-Yoon Lee[b,c,2], and Insung S. Choi[a,b,c,d,2]

[a]Center for Cell-Encapsulation Research, [b]Molecular-Level Interface Research Center, and Departments of [c]Chemistry and [d]Bio and Brain Engineering, Korea Advanced Institute of Science and Technology (KAIST), Daejeon 305-701, Korea; [e]Division of Life Science, Korea Basic Science Institute, Daejeon 305-806, Korea; [f]SKKU Advanced Institute of Nanotechnology, Sungkyunkwan University, Suwon 440-746, Korea; and [g]School of Materials Science and Engineering, Gwangju Institute of Science and Technology, Gwangju 500-712, Korea

Edited by Robert Langer, Massachusetts Institute of Technology, Cambridge, MA, and approved December 16, 2014 (received for review October 14, 2014)

The posttranslational modification of neural cell-adhesion molecule (NCAM) with polysialic acid (PSA) and the spatiotemporal distribution of PSA-NCAM play an important role in the neuronal development. In this work, we developed a tissue-based strategy for metabolically incorporating an unnatural monosaccharide, peracetylated *N*-azidoacetyl-D-mannosamine, in the sialic acid biochemical pathway to present *N*-azidoacetyl sialic acid to PSA-NCAM. Although significant neurotoxicity was observed in the conventional metabolic labeling that used the dissociated neuron cells, neurotoxicity disappeared in this modified strategy, allowing for investigation of the temporal and spatial distributions of PSA in the primary hippocampal neurons. PSA-NCAM was synthesized and recycled continuously during neuronal development, and the two-color labeling showed that newly synthesized PSA-NCAMs were transported and inserted mainly to the growing neurites and not significantly to the cell body. This report suggests a reliable and cytocompatible method for in vitro analysis of glycans complementary to the conventional cell-based metabolic labeling for chemical glycobiology.

metabolic labeling | bioorthogonal reaction | polysialic acid | 1,3-dipolar cycloaddition | primary hippocampal neuron

The spatial distribution and chemical composition of diverse surface glycans contain crucial information on the physiological and functional states of cells (1). The glycans modulate a multitude of cellular functions, such as adhesion, differentiation, cell–cell interactions, and recognition of external molecules, by mediating intracellular signaling events and also, intercellular communications (2, 3). The regulatory functions of glycans are also considered to be significant in neurons, and previous biological work has suggested the intimate involvement of glycosylation in neurite development, synaptic plasticity, and neural regeneration (4–7). The functional modulation of neural cell-adhesion molecule (NCAM) with polysialic acid (PSA), in particular, has been a primary target in the investigation of glycan roles in neurons. PSA is an α2,8-linked linear polysaccharide composed of up to 200 sialic acids and shown to inhibit the homophilic and heterophilic interactions between NCAMs in a reversible manner (8). The polysialylation of NCAM, a unique posttranslational modification in nervous systems, is most prominent during the early developmental stages and attenuated gradually after birth as the nerve systems mature and the cellular contacts become stabilized (9). PSA-NCAMs occasionally remain until adulthood in the brain regions that exhibit plasticity, including hippocampus, and they are reported to be involved in glia–neuron interactions, regulation of circadian rhythms, and learning and memory (10). Other than these roles, PSA is closely related to the tumor progression of malignant neuroblastoma (11, 12). However, despite the widespread occurrence of PSAs and their biological complexity in the nerve systems, the PSA-mediated modulation of neuronal functions is not fully understood. Thus, de novo imaging and tracing of the spatiotemporal distribution of PSAs in neurons at the early stages of neuronal development (e.g., neuritogenesis) would be extremely helpful to elucidate the multidimensional roles of PSAs in neurite development and synapse formation.

Bioanalytical techniques for studying glycans are not as straightforward as those for doing DNA and proteins. The biosynthesis of glycans is not genetically encoded, which makes their imaging or quantitative analysis extremely hard with conventional biochemical methods (13, 14). In addition, the glycans markedly vary in structure (oligosaccharides, glycolipids, and peptidoglycans), and each oligosaccharide chain has multiple linkage types along with intricate stereochemistry. In this regard, the use of unnatural synthetic monosaccharides in the cellular glycosynthetic pathway has been proposed as an alternative method for overcoming the aforementioned limitations in the glycan analysis. This metabolic approach stemmed from the early work by Reutter and coworkers (15–18), who used the *N*-acyl derivatives of *N*-acetyl-D-mannosamine (ManNAc) and *N*-acetyl-D-glucosamine in in vitro and in vivo metabolic synthesis of sialic acids to investigate the biological effects of incorporated unnatural sialoglycoconjugates. *N*-propanoyl-D-mannosamine (ManNProp), differing from natural ManNAc by an additional methylene (CH_2) group, has intensively been used and applied to neuroblastoma, nonneuronal glia, and

Significance

The roles of cell-surface glycans remain elusive compared with those of proteins or lipids because of their diverse and dynamic nature. Metabolic incorporation of unnatural monosaccharides in the biochemical synthesis of glycans as a chemical reporter has been a successful method to investigate the functions of cell-surface glycans but has also left an issue of cytotoxicity for certain cells. In this work, we developed a tissue-based strategy for metabolic incorporation of a chemical reporter to primary neurons. We let an unnatural monosaccharide be metabolized by hippocampal tissues before dissociation into individual cells, and thereby, we could eliminate cytotoxicity. We used this method to describe, for the first time to our knowledge, the real-time distribution of polysialic acids on the membranes of neurons.

Author contributions: K.K., S.J., and I.S.C. designed research; K.K., S.J., and J.Y.C. performed research; S.G., S.-P.H., S.-Y.L., Y.H.K., and S.-M.K. contributed new reagents/analytic tools; K.K., S.J., J.Y.C., M.-H.Y., Y.N., K.-B.L., H.-Y.L., and I.S.C. analyzed data; and K.K., S.J., J.Y.C., and I.S.C. wrote the paper.

The authors declare no conflict of interest.

This article is a PNAS Direct Submission.

[1]K.K., S.J., and J.Y.C. contributed equally to this work.

[2]To whom correspondence may be addressed. Email: ynam@kaist.ac.kr, kblee@kbsi.re.kr, leehy@kaist.ac.kr, or ischoi@kaist.ac.kr.

This article contains supporting information online at www.pnas.org/lookup/suppl/doi:10.1073/pnas.1419683112/-/DCSupplemental.

cerebellar cells (11, 12). On the other hand, Bertozzi and coworkers (19–22) metabolically introduced monosaccharide-based chemical reporters—*N*-acyl derivatives of ManNAc, *N*-acetyl-D-glucosamine, or *N*-acetyl-D-galactosamine containing a ketone or azide group—onto cellular surface glycans followed by bioorthogonal, chemoselective coupling with a fluorescent dye or an affinity tag bearing hydrazide/aminooxy (for ketones) or phosphine/alkyne (for azides) group. This elegant methodology, combining metabolic engineering and bioorthogonal reactions, enabled in situ imaging or proteomic enrichment of one glycan type (19–22) and has been applied to many different cell lines (e.g., Jurkat, HeLa, CHO, and neuron-like blastoma cells) and organisms (e.g., zebrafish, mice, and microbes) for the selective labeling of sialic acid (23–25), *N*-acetyl-D-galactosamine residue (in mucin-type *O*-linked glycan) (26–28), fucose residue (29–32), and LPSs/*O*-antigen (33, 34). Although there are innumerable previous reports, the metabolic labeling and the imaging of glycan structures in primary neurons have yet to be achieved, although the surface glycans, especially PSA-NCAMs, play important roles in neuronal development.

In this report, we suggest a tissue-based strategy for metabolically introducing unnatural monosaccharides to primary hippocampal neurons. The modification of the metabolic methods was required for the primary neurons because of the incompatibility of the previously reported method with the hippocampal neurons: we found that a commonly used monosaccharide for metabolic labeling—peracetylated *N*-azidoacetyl-D-mannosamine (Ac_4ManNAz)—had a dose-dependent inhibitory effect on neurite outgrowth and ultimately, caused cell death when it was fed to cultured neurons (detailed data are in *Results* and *Discussion*). The adverse effects of Ac_4ManNAz disappeared when it was metabolized by hippocampal tissues [this method is denoted as the metabolism-by-tissues (MbT) method here to be differentiated from the conventional metabolism-by-cells (MbC) method]. The MbT method enabled the stable, simultaneous de novo tracing of PSA-NCAMs in neurons after copper(I)-catalyzed azide-alkyne cycloaddition (CuAAC) reactions with fluorescent alkynes. This tissue-based strategy for metabolically labeling sialic acids in primary hippocampal neurons, we believe, would give a versatile tool for investigating the PSA-mediated dynamic regulation of neurite and synaptic developments.

Results

MbC Method for Metabolic Labeling: Effects of Ac_4ManNAz on Neuronal Development and Viability. Nervous systems are composed of multiple types of neurons and glial cells (e.g., astrocytes, oligodendrocytes, and microglia in the CNSs). Neurons develop neurites (axons and dendrites) and have a capacity to generate action potentials; glial cells mainly fulfill supportive or regulative functions for neuronal development or synaptic transmission. Therefore, labeling the sialoglycoconjugates of neurons, not glial cells, with unnatural reporter monosaccharides would provide direct information on the PSA roles in neuronal developments and functions. In particular, in this study, we chose primary hippocampal neurons for metabolic labeling of PSA-NCAMs, because the primary culture would make it possible to follow the important neuronal developments from the early stage, including neuritogenesis, by metabolic engineering. PSA is found in the hippocampal region of the brain and responsible for the tasks related to learning and memory, even during adulthood (35), which would allow for study on the spatial and temporal distributions of PSA-NCAMs.

To introduce the azide moiety to sialoglycoconjugates in neurons by the MbC method, primary hippocampal neuron cells (50–200 cells/mm^2) were cultured in the presence of Ac_4ManNAz (Fig. 1*A*) [intracellular metabolic processes of Ac_4ManNAz have previously been reported (17)]. Briefly, the neurons, after dissociated from the hippocampal tissues of embryonic day 18 (E18) Sprague–Dawley rats, were seeded on a poly-D-lysine–coated glass coverslip in Neurobasal medium with B-27 supplement, to which was added a DMSO solution of Ac_4ManNAz (10 mM) at a final concentration of 50 μM.

After 2 d of feeding, the neurons were reacted with Alexa Fluor 594 alkyne (25 μM) and immediately observed without fixation. In other words, the Ac_4ManNAz feeding was performed at 0 d in vitro (DIV), and the CuAAC reaction was performed at 2 DIV. For the CuAAC reaction, a recently developed ligand, 2-[4-{{bis[(1-*tert*-butyl-1*H*-1,2,3-triazol-4-yl)methyl]amino}methyl}-1*H*-1,2,3-triazol-1-yl]acetic acid (36–38), was used to minimize the cytotoxicity of Cu(I) ions and fasten the coupling reaction (39). After a 5-min reaction at 4 °C, the intense red fluorescence was observed at the entire cellular surface, including neuronal cell bodies (somas) and neurites (Fig. 1*B* and Fig. S1). In particular, lamellipodial and filopodial structures at the tips of growing neurites were labeled with remarkable intensity. Fluorescence was not observed in the cases omitting either the Ac_4ManNAz feeding or the CuAAC reaction (Fig. S2), indicating that the labeling was purely the result of metabolic incorporation of Ac_4ManNAz and subsequent coupling reaction.

Although ManNAc derivatives are tolerated and metabolized by most cell lines, reports on their cytotoxicity are also found, especially for neuron-like cells (40). For example, the growth rate of NG108-15 neuroblastoma-glioma hybrid cells was slowed sharply by feeding of 1 mM *N*-glycolyl-D-mannosamine pentaacetate, and the cell viability decreased to 76% after 70 h of feeding (11). In addition, 0.1 mM peracetylated ManNAc (Ac_4ManNAc) derivatives were reported to be toxic to terminally differentiated human embryonic carcinoma NT2 cells (41). Although ManNProp (5 mM) was not cytotoxic, it altered the fate of cerebellar neurons in the microexplant culture containing neurons and glial cells (42). *N*-butanoyl-D-mannosamine (10 mM; 48 h) reduced proliferation of human B-lymphoma and monkey kidney epithelium cell lines by 30–40%, whereas ManNProp did not (43). These previous reports clearly indicated that the cytotoxicity of unnatural ManNAc derivatives was monosaccharide- and cell line-dependent, necessitating the cytotoxicity test for primary hippocampal neurons in our system.

In the MbC method, the neurite development was found to be suppressed greatly by the Ac_4ManNAz feeding (50 μM) (Fig. 1*C*). At 2 DIV, the average length of the longest neurites was 62.8 ± 2.0 μm for the neurons that were cultured without Ac_4ManNAz (normal culture; control), but the length decreased greatly to 25.3 ± 0.6 μm for the Ac_4ManNAz-metabolized neurons (Fig. 1*D*). The feeding of hippocampal neurons with Ac_4ManNAc (*SI Text* discusses the synthesis of Ac_4ManNAc) also caused a decrease in the neurite length to 31.8 ± 2.8 μm. The adverse effect of Ac_4ManNAz in the neuronal development was dose-dependent (Fig. 1*E*). For example, twofold increase in the Ac_4ManNAz concentration (100 μM) abrogated the neuritogenesis completely, and no neurites were observed, whereas the fluorescence intensity was proportional to the Ac_4ManNAz concentration as expected. This result might be on the same line with a recent finding that PC12 cells developed neurites with treatment of ManNProp or ManNAc (5 mM; 120 h) in the absence of nerve growth factor, presumably implying the involvement of sialic acid metabolism in gene expression and cell differentiation, although the phenotypic consequences were opposite to each other (44, 45). Whereas ManNProp induced the neurite outgrowth of neuron-like PC12 cells, Ac_4ManNAz suppressed the neurite outgrowth of primary hippocampal neurons.

Not only did Ac_4ManNAz suppress the neurite development, but it also caused cell death in the MbC-based feeding. The viability of the Ac_4ManNAz-metabolized neurons (50 μM) was 43.5% at 2 DIV but sharply dropped to 3.75% at 3 DIV and 1.23% at 4 DIV (Fig. 1*F*). The live-cell imaging showed that the neurites decomposed gradually, and then, the somas were detached from

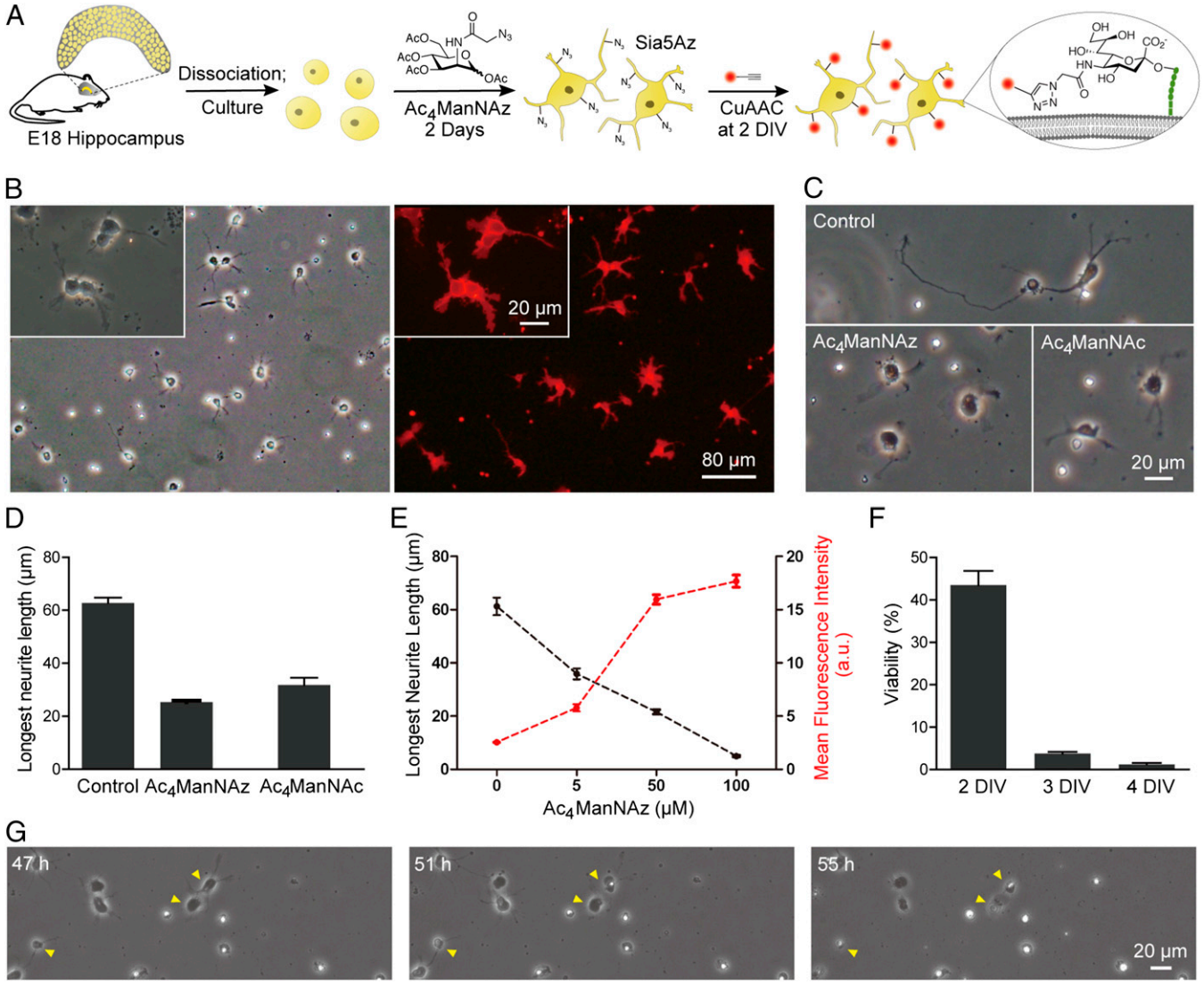

Fig. 1. Dose-dependent cytotoxicity of Ac_4ManNAz in the MbC method. (*A*) Schematic illustration of the MbC procedure. (*B*) Phase-contrast and fluorescence micrographs of Sia5Az-presenting neurons after CuAAC reaction with Alexa Fluor 594 alkyne (red). (*Inset*) Images with a higher magnification. (*C*) Phase-contrast micrographs of neurons at 2 DIV. Control indicates the neurons after 2 d of normal culture, Ac_4ManNAz indicates the neurons after 2-d feeding of Ac_4ManNAz, and Ac_4ManNAc indicates the neurons after 2-d feeding of Ac_4ManNAc. (*D*) Average lengths (means ± SEs) of the longest neurites at 2 DIV. (*E*) Dose-dependent effects of Ac_4ManNAz on the lengths of the longest neurites and the fluorescence intensity. (*F*) Viabilities of the neurons fed with Ac_4ManNAz for 2 d. (*G*) Phase-contrast micrographs of Ac_4ManNAz-fed neurons at 47, 51, and 55 h in vitro. The images were taken from the live-cell imaging data (Movie S1). E18 Hippocampus: Hippocampus from embryonic day 18 (E18) Sprague–Dawley rats.

the surface, leaving debris of dead cells (Fig. 1*G* and Movie S1 show the live-cell imaging data). The addition of DMSO or Cu(I) to the culture medium did not cause the cell death, eliminating the cytotoxic effects of DMSO or Cu(I) (Fig. S3). Taken together, our results, along with previous ones by others, implied that the cellular activities and viability were affected when the feeding of ManNAc derivatives was performed at the cultured cell level, although additional investigation would elucidate the biochemical implications of these observed phenomena. In any case, the metabolic labeling shown in Fig. 1*B* would not faithfully manifest the natural, unperturbed development of primary hippocampal neurons, requiring new methods for labeling sialoglycoconjugates of the neurons.

MbT Method for Metabolic Labeling: Feeding Ac_4ManNAz to Hippocampal Tissues. The adverse effects of Ac_4ManNAz on cultured neurons possibly allowed only for the analysis of temporally fixed distribution of sialic acid residues to some extent but not for in situ dynamic imaging of individual living neurons. We envisioned that the primary neurons would tolerate external perturbations better when they were interconnected to each other and supplemented by tissue scaffolds and nutrients. Our hypothesis was supported indirectly by a previous report, in which ManNProp, a potent inhibitor of a polysialyltransferase (ST8SiaII) (41, 46), was metabolized and expressed on cell membranes in hippocampal slice culture and in vivo, although at an extremely low efficiency, probably by another polysialyltransferase (ST8SiaIV) (7, 47). The use of tissue culture was also hinted as a means of increasing the cellular tolerance to unnatural sialic acids and their precursors, although no data were presented (43).

In the MbT method, a freshly dissected hippocampal tissue was fed with Ac_4ManNAz before dissociation for neuron culture. To confirm the plausibility of the MbT strategy, we first incubated hippocampal tissues in culture medium without Ac_4ManNAz for

2 d. The neurons from the tissues, after 2 d of incubation and subsequent dissociation, survived and developed as normally as the neurons without tissue incubation (the control). Based on this observation, we fed Ac_4ManNAz to dissected hippocampal tissues for 2 d and subsequently dissociated the tissues into individual neurons for plating (Fig. 2*A*). In some cases, large tissues were torn apart into several smaller pieces before Ac_4ManNAz feeding. The day of plating was counted to be 0 DIV. In stark contrast to the feeding of Ac_4ManNAz to cultured neurons in the MbC method, its feeding to hippocampal tissues did not suppress neurite development or cause the cell death compared with the control. Fig. 2*B* showed that there was no statistical difference in the longest neurite length between the MbT method and the control at 1 DIV. In addition, the viability was also comparable with that of the control at 30 min after plating and did not decrease afterward (Fig. 2*C*). The Ac_4ManNAz-fed neurons continuously survived well and developed into a mature, well-connected neuronal network (Fig. S4).

Spatial Distribution of PSA-NCAM. The formation of *N*-azidoacetyl sialic acid (Sia5Az) from Ac_4ManNAz and its incorporation into sialoglycoconjugates as PSA were first investigated, because previous reports did not give one consistent trend in metabolic incorporation of unnatural monosaccharides into PSA. Bertozzi and coworkers (48) used NT2 cells for PSA modulation and found that *N*-levulinoyl-D-mannosamine (ManLev) was effectively incorporated into the outer segment of PSA and that the ManLev treatment did not have any negative impact on the development of NT2 cells, even with 3 mM ManLev. However, Bertozzi and coworkers (48) also reported that the surface PSA expression in NT2 cells was reversibly inhibited by *N*-butanoyl-D-mannosamine but not by ManNProp (46). ManNProp was successfully applied to the mixed glial cell culture (42), but the PSA synthesis was found to be greatly suppressed by the ManNProp treatment in hippocampal slice culture (7). These rather scattered examples also indicated that the metabolic incorporation of unnatural monosaccharides into PSA (and their cytotoxicity) was cell- and substrate-dependent. In our case, the Western blot analysis showed that the Ac_4ManNAz (50 μM) feeding did not suppress or inhibit the PSA synthesis (Fig. 2*D*). A hippocampal tissue with or without Ac_4ManNAz feeding was homogenized, and the proteins from each tissue were analyzed with anti–PSA-NCAM by gel electrophoresis. The quantity of PSA-NCAM in the MbT method was comparable with that of the control. In addition, the sialidase A-catalyzed cleavage of PSA-NCAM also confirmed the unaltered synthesis of sialic acid and the formation of PSA-NCAM.

In the primary neuron culture, right after plating (within 1 h), the majority of neurons have only lamellipodia, and a few of them sprout several short neurites (49). The neurons, dissociated from Ac_4ManNAz-fed tissues in the MbT method, showed this normal morphological trend (Fig. 2*E*). The metabolic incorporation of Ac_4ManNAz in the hippocampal tissues was confirmed by the CuAAC reaction with Alexa Fluor 594 alkyne within 1 h after plating. The cells were analyzed without fixation, such as in the MbC method. We observed intense red fluorescence throughout the entire cell structures, indicating the successful labeling of PSA-NCAM. The spatial distribution of

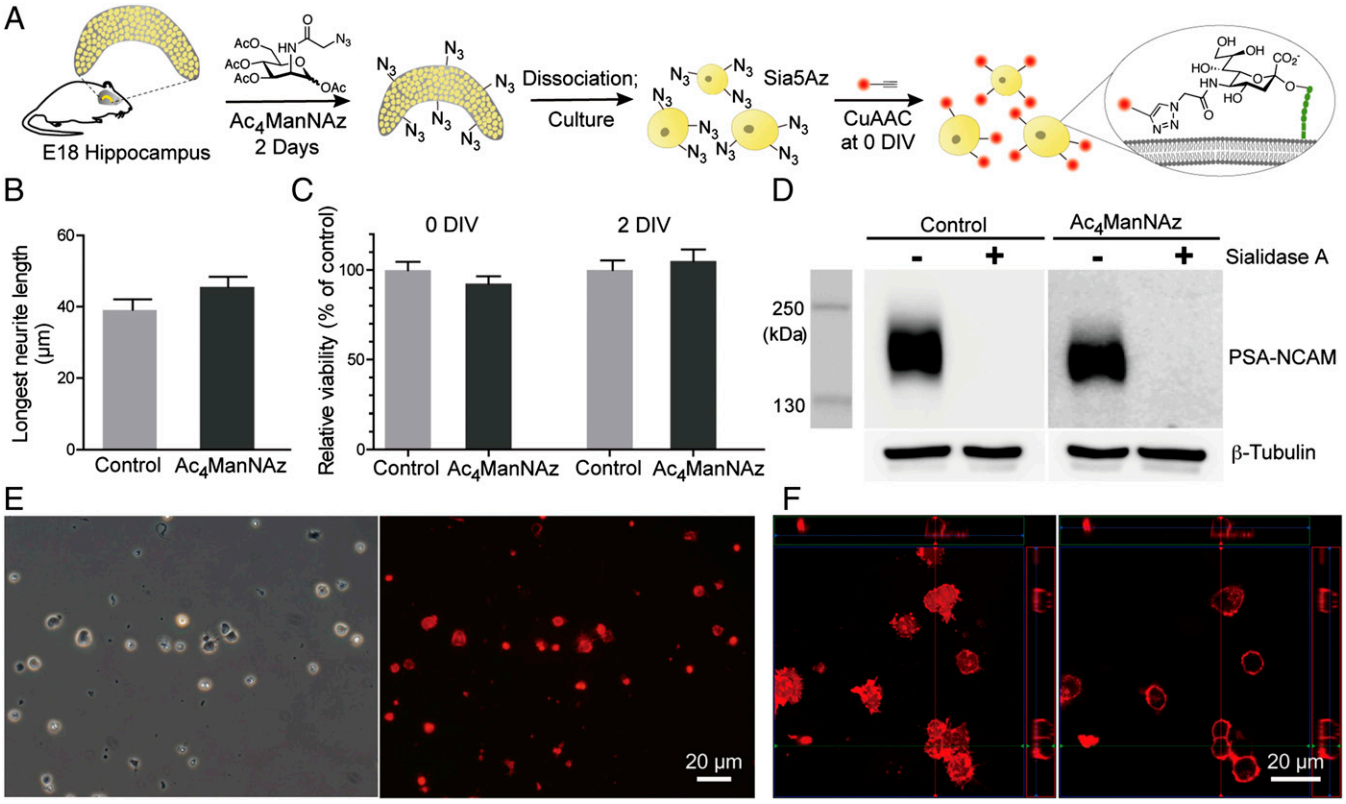

Fig. 2. Neurocompatibility of the MbT method. (*A*) Schematic illustration of the MbT procedure. (*B*) Average lengths (means ± SEs) of the longest neurites at 1 DIV. Control indicates the neurons dissociated from the tissues that were cultured normally for 2 d, and Ac_4ManNAz indicates the neurons dissociated from the tissues that were cultured with 50 μM Ac_4ManNAz. (*C*) Relative viabilities of Sia5Az-presenting neurons at 30 min after plating (0 DIV) and at 2 DIV. (*D*) Western blot analysis of tissue lysates. (*E*) Phase-contrast and fluorescence micrographs of neurons at 0 DIV after reacting with Alexa Fluor 594 alkyne (red). (*F*) Confocal laser-scanning microscopy images of neurons at 0 DIV after reacting with Alexa Fluor 594 alkyne. The images were obtained in (*Left*) lower and (*Right*) upper *Z* planes, respectively. E18 Hippocampus: Hippocampus from embryonic day 18 (E18) Sprague–Dawley rats.

PSA-NCAM was investigated by *Z*-resolved confocal fluorescence microscopy (Fig. 2*F*). The fluorescence images showed that PSA-NCAM existed at F-actin–based protrusions (lamellipodia and filopodia) as well as the somas and minor neurites. The red fluorescence was detected for all of the neurons investigated, confirming that the MbT method was neurocompatible and effective in visualizing PSAs with high fidelity.

Temporal Distribution of PSA-NCAM. The distribution of surface glycans is not static but rather, constantly varying, because the glycans often work as dynamic regulators for protein functions according to each biological context. In addition, the insertion site of membranes and their components (e.g., proteins and lipids) during axonal growth is still inconclusive (50), although intensive work has been done since the first report in 1970 (51).

In the neuronal development, the dynamics of PSA-NCAMs (formation and distribution) are involved intimately in neuritogenesis, neurite outgrowth, and axon formation (6, 52). To gain insight into the temporal fate of PSA-NCAMs, we labeled the Sia5Az-presenting PSA-NCAMs with red fluorescent Alexa Fluor 594 alkyne at 0 DIV (within 1 h of plating) and observed the same cells at the predetermined times (0, 1, 3, and 7 DIV) (Fig. 3*A*). The time-lapse fluorescence images showed that the fluorescence intensity at the soma gradually decreased with time, and a weak intensity was barely observed at the growing neurites. Because we stopped the Ac_4ManNAz feeding after plating, the decrease in the fluorescence intensity at the soma indicated that PSA-NCAMs continued to be formed during the early stages of neuronal developments, and the Sia5Az-presenting PSA-NCAMs were replaced with the newly formed PSA-NCAMs (the ones that did not have the azide groups and the Sia5Az-presenting PSA-NCAMs). The very weak fluorescence intensity at the neurites also implied that the dynamic but passive distribution of the preformed PSA-NCAMs on the cell membranes did not occur significantly. In addition, we tried to label the Sia5Az-presenting PSA-NCAMs from different samples at different time points (1, 3, 7, and 10 DIV) and imaged them right after each labeling (Fig. 3*B*). The spatiotemporal distribution and relative intensity of the Sia5Az-presenting PSA-NCAMs were in a good agreement with the results of the time-lapse imaging.

The neuritogenesis and neurite outgrowth of hippocampal neurons in culture are highly active within 1 DIV, and the neuronal polarity is observed at 2–3 DIV (49). Accordingly, PSA-NCAM is known to be prevalent in the initial stages of neuronal development, and its surface density gradually decreases as the neurons mature, because it helps the neurons migrate or the neurites elongate by reducing cell–cell adhesiveness (10). The neurons were labeled with red fluorescent Alexa Fluor 594 alkyne right after plating or at 1 DIV followed by a second labeling with a green fluorescent tag (Alexa Fluor 488 alkyne) at 1 or 3 DIV (Fig. 4). In this manner, red and green fluorescence corresponded to the Sia5Az-presenting PSA-NCAMs formed at the neuron surfaces earlier and later, respectively.

During the first day after plating, neurons generally sprout several minor neurites, one of which markedly elongates and becomes an axon, whereas the others become dendrites. Therefore, the relative fluorescence intensity would give the information on the dynamic and temporal membrane distribution of PSA-NCAMs. At 1 DIV, red fluorescence was observed with

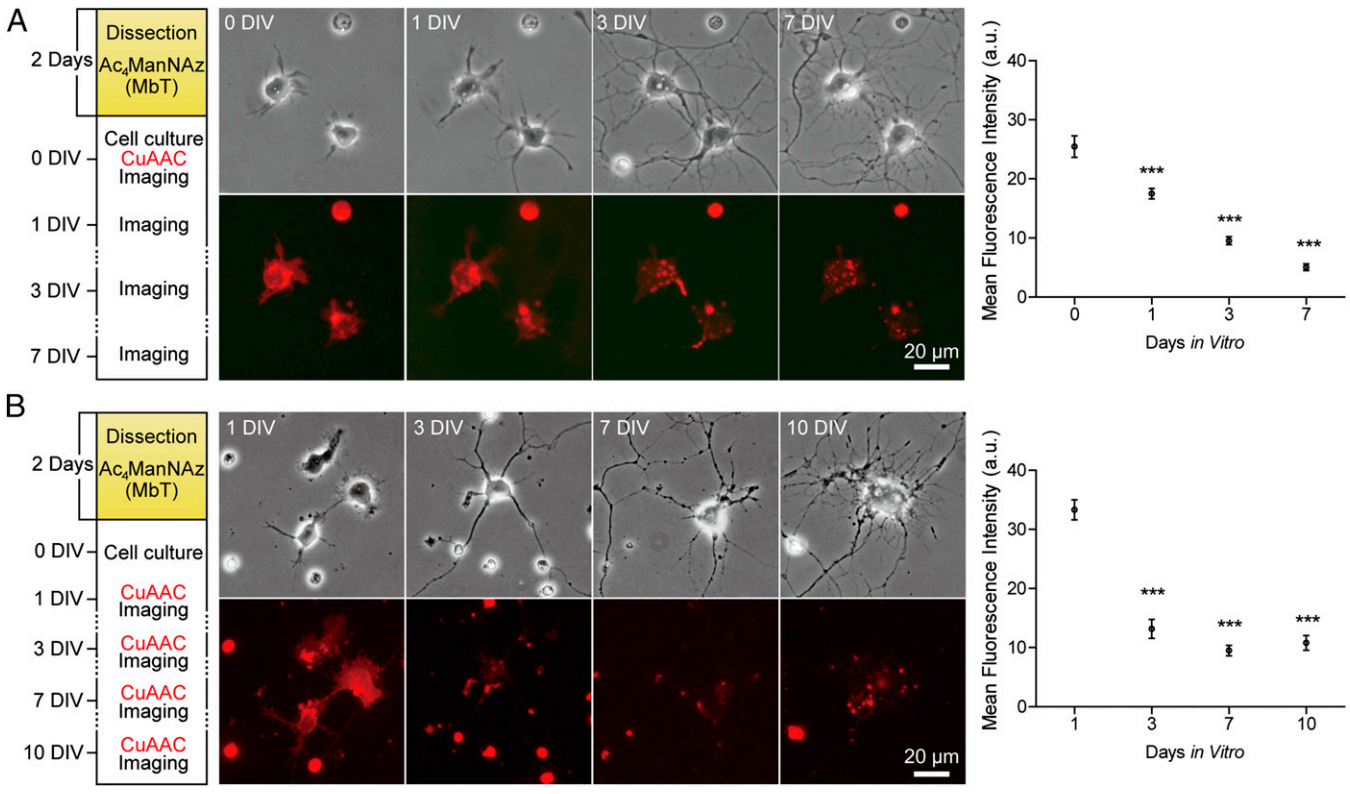

Fig. 3. Temporal analysis of PSA-NCAM in the primary culture of hippocampal neurons. (*A*, *Left*) Phase-contrast and fluorescence micrographs of Sia5Az-presenting neurons in the MbT method. The cells were reacted with Alexa Fluor 594 alkyne at 0 DIV and observed at 0, 1, 3, and 7 DIV. (*A*, *Right*) Average fluorescence intensities of the soma areas at each time point. ***$P < 0.001$. (*B*, *Left*) Phase-contrast and fluorescence micrographs of Sia5Az-presenting neurons in the MbT method. Each sample was reacted with Alexa Fluor 594 alkyne at 1, 3, 7, or 10 DIV and observed right after each reaction. (*A*, *Right*) Average fluorescence intensities of the soma areas at each time points. ***$P < 0.001$.

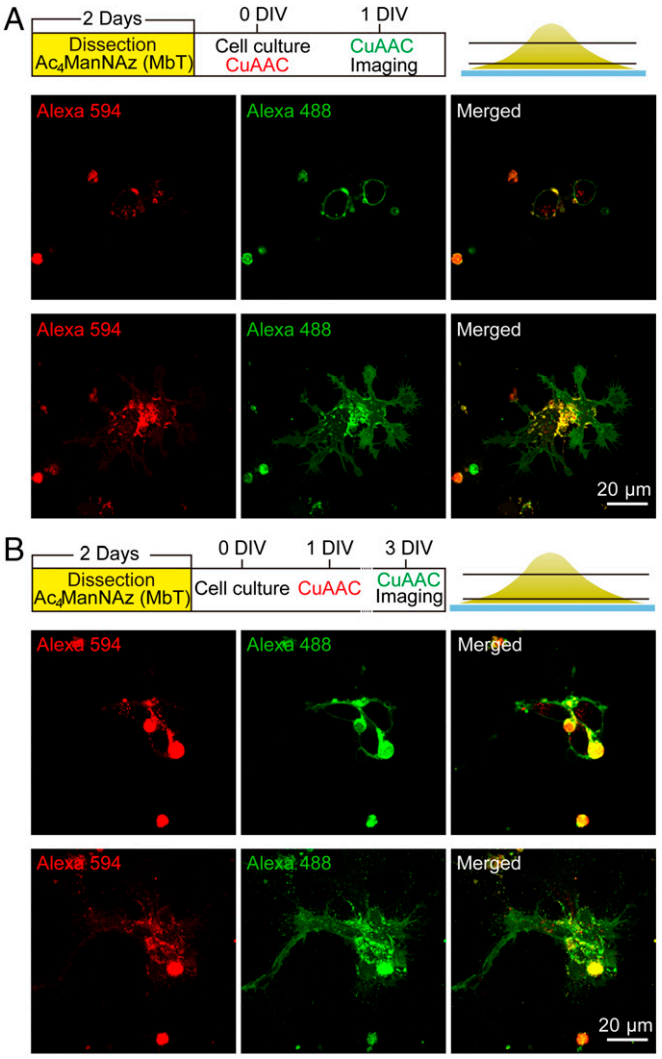

Fig. 4. Two-color labeling of PSA-NCAM. Confocal laser-scanning microscopy images [(*Upper*) higher *Z* plane; (*Lower*) lower *Z* plane] of Sia5Az-presenting neurons in the MbT method. (*A*) The neurons were dual-labeled by two successive CuAAC reactions with Alexa Fluor 594 alkyne (red) at 0 DIV and Alexa Fluor 488 alkyne (green) at 1 DIV. The images were taken at 1 DIV. (*B*) The neurons were dual-labeled by two successive CuAAC reactions with Alexa Fluor 594 alkyne (red) at 1 DIV and Alexa Fluor 488 alkyne (green) at 3 DIV. The images were taken at 3 DIV.

high intensity mainly at the somas; relatively low intensity of red fluorescence was detected at the developing minor neurites in the confocal laser-scanning microscopy images (Fig. 4*A*). In contrast, green fluorescence was observed throughout the cell surfaces, including somas and neurites. The results strongly implied that the site of PSA-NCAM incorporation would be the growing tips and not the cell body: the Golgi-derived PSA-NCAM was synthesized in the soma and transported anterogradely through a membrane vesicle to the growth cones. Information in Fig. 4*A* also suggests the occurrence of a retrograde movement of PSA-NCAMs in membranes and its recycling. The confocal laser-scanning microscopy images focused on a higher *Z* plane (Fig. 4 *A*, *Upper* and *B*, *Upper* and Movies S2 and S3 show the combined full *z*-axis images) showed that significant amounts of the presynthesized PSA-NCAMs (red in Fig. 4 *A*, *Upper* and *B*, *Upper*) were relocated into a cytoplasm, whereas the fresh PSA-NCAMs (green in Fig. 4 *A*, *Upper* and *B*, *Upper*) existed only on cell membranes, indicating the presence of intracellular machinery for turnover of PSA-NCAMs. The same phenomena were also observed with the neuron cells after labeling at 1 and 3 DIV (Fig. 4*B*).

Because of its cytotoxicity, the MbC method could be used to label the PSA-NCAM present at certain time points. We combined the two methods (MbC and MbT) to further characterize the temporal distribution of PSA-NCAMs within 1 DIV, with additional feeding of Ac_4ManNAz to the cultured neurons. After reacting with Alexa Fluor 594 alkyne right after plating (MbT method), the neurons were cultured for 1 d in a medium containing Ac_4ManNAz (50 μM) and labeled with Alexa Fluor 488 alkyne at 1 DIV (Fig. S5). The fluorescence intensities for both red and green were enhanced because of additional synthesis of Sia5Az. In the fluorescence microscopy images, neurites (and filopodia) were clearly seen in green (Fig. S5*B*).

PSA-NCAM in the Neuronal Network. The MbC methods could be used for the characterization of the late stages in the neuronal development. We labeled PSA-NCAMs in the in vitro hippocampal neuronal networks at relatively matured phases by feeding Ac_4ManNAz directly to the cultures at 10 DIV. Neurons at 10 DIV form a dense network throughout the entire substrate with many neurite processes, and the 2-d feeding was found not to significantly destroy the network structure (Fig. S6). The newly synthesized PSA-NCAMs were distributed throughout the entire network, including somas and neurites. Higher fluorescence intensity was measured from the clustered somas, indicating that the role of PSA-NCAM in cell–cell adhesiveness remained effective at later stages of neuronal development. In addition, astrocytes were reported to emerge in the long-term, serum-free culture of primary hippocampal neurons (53), which was investigated by immunostaining astrocytes after labeling PSA-NCAMs (Fig. 5). The colocalization study showed that the majority of astrocytes were colocalized with PSA-NCAM, implying the involvement of PSA in regulating the interaction between neurons and glial cells in matured networks (54).

Discussion

Compared with other biological systems, the current understanding of the functions of nerve systems is disappointingly deficient. Nerve systems are inherently difficult to untangle, because (*i*) most of their functions are based on the transient and dynamic interactions that are difficult to track in a complex network of neurons and (*ii*) the roles of each type of neuron vary significantly depending on their developmental context. In light of these challenges, the heterogeneity of glycans and their regulatory roles in multiple biological functions suggest that they could be invaluable components for characterizing nerve functions, and the importance of glycans in brain development, neuroregeneration, and synaptic plasticity strongly supports this notion. Therefore, the development of a method that can analyze the dynamics of glycan activity in neurons would be of significant value to any research that seeks to decode neural functions.

We believe that the tissue-based feeding method for metabolically labeling the cell-surface glycans (the MbT method) presented in this paper is a compelling candidate to make remarkable advances in glyconeurobiology. With Ac_4ManNAz as a model of unnatural monosaccharides, we successfully tracked the temporal and spatial distribution of PSA-NCAMs at the early stages of neuronal development. The neurocompatibility is one of the prominent advantages of the MbT method compared with the conventional cell-based feeding method. Interestingly, neurons (and also, neuron-like cells) are found to be more susceptible to unnatural ManNAc derivatives than other mammalian cell types. Although biochemical explanation remains to be seen, the

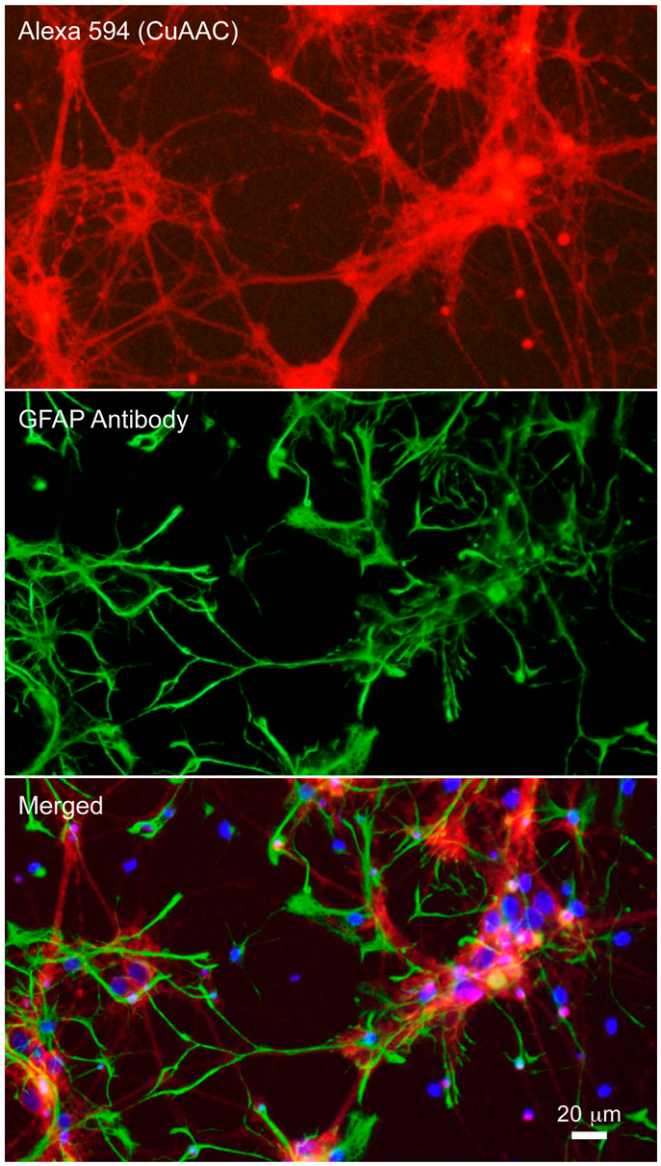

Fig. 5. PSA-NCAM in the matured neuronal network. Fluorescence micrographs of the Sia5Az-presenting cells in the MbC method at 12 DIV. The neurons were fed with Ac_4ManNAz (50 μM) at 10 DIV for 2 d followed by reacting with Alexa Fluor 594 alkyne (red) and immunostaining with anti-GFAP antibodies (green) and Hoechst 33342 (blue).

cytotoxicity of ManNAc derivatives would be the circumstantial evidence that the sialic acid synthesis pathway is incomparably crucial and therefore, tightly controlled in neurons. The issues in the cytotoxicity are not understood completely, but the MbT method would be a practical alternative to the conventional MbC method. The MbT method allowed us to label the PSA-NCAMs in the cultured hippocampal neurons de novo and showed that the neurons constantly synthesized PSA-NCAM, which was added mainly to the newly developing regions. However, the MbC method also could be used to image PSA-NCAMs at the fixed time points, although cell death (and morphological changes) prevented us from following their temporal distributions. The imaging of PSA-NCAMs at 12 DIV indicated that sialic acid kept synthesizing in neurons (and astrocytes) in the matured neuronal network. We believe that the tissue-based method shown with hippocampal tissues in this report will be readily applied to other tissues, such as cortical tissues (Fig. S7).

Methods

Cell Culture. Primary hippocampal neurons were cultured in serum-free conditions. The hippocampus from an E18 Sprague–Dawley rat was triturated in 1 mL HBSS (Welgene) using a pipette. The cell suspension was centrifuged for 2 min at 611 × *g*, and a cell pellet was extracted. The cell pellet was suspended in Neurobasal medium (Gibco) supplemented with B-27 (Invitrogen), 2 mM GlutaMAX (Gibco), 12.5 μM L-glutamic acid (Sigma), and 1% penicillin-streptomycin (Gibco). Dissociated cells were seeded at a density of 50–200 cells/mm^2 on glass coverslips (18 mm in diameter; Marienfeld), which were coated with poly-D-lysine (0.1 mg/mL in deionized water; Sigma) for 1 h. Cultures were maintained in an incubator [5% (vol/vol) CO_2 and 37 °C], and one-half of the medium was replaced with fresh culture medium without L-glutamic acid supplement every 3–4 d. This study was approved by the Institutional Animal Care and Use Committee of Korea Advanced Institute of Science and Technology (KAIST).

Metabolic Labeling of Cell-Surface PSAs. To feed a monosaccharide to neurons by the MbC method, cells were plated on glass coverslips with a density of 50–200 cells/mm^2 and grown with or without 10–100 μM Ac_4ManNAz (Thermo Scientific) or Ac_4ManNAc for 2 d. The medium was gently aspirated, and the cells were washed twice with 1 mL PBS (Gibco). In the case of the MbT method, hippocampal tissues were incubated in the medium containing the monosaccharides before they were dissociated and cultured on glass coverslips. For the CuAAC reaction, $CuSO_4$ (50 μM) and 2-(4-((bis((1-(*tert*-butyl)-1*H*-1,2,3-triazol-4-yl)methyl)amino)methyl)-1*H*-1,2,3-triazol-1-yl)acetic acid [250 μM; synthesized by following the reported procedures (55, 56)] in a 1:5 molar ratio were added at 4 °C to PBS containing Alexa Fluor 594 alkyne or Alexa Fluor 488 alkyne (25 μM; both from Life Technologies) and aminoguanidine (1 mM; Sigma). A freshly prepared stock solution of sodium ascorbate (100 mM; Sigma) was added to the resulting solution to establish a final ascorbate concentration of 2.5 mM. This reaction mixture was incubated for 10 min at 4 °C and then added to the cells followed by incubation at 4 °C for 5 min. After the reaction, the cells were washed three times with PBS and observed with a microscope. For dual labeling, the cells were washed with PBS after the first labeling and placed in a medium containing 50 μM Ac_4ManNAz for another 1 d.

Proteomic Analysis of PSAs in the Hippocampus Fed with Ac_4ManNAz. The sample, a hippocampus or an Ac_4ManNAz-fed hippocampus, was homogenized in a mammalian protein extraction buffer (GE Healthcare) and incubated on ice for 1 h. The homogenates were then centrifuged, the supernatants were collected, and total protein concentration was determined according to the Bradford assay procedure (Bio-Rad) by using BSA as a standard; 20 μg each protein sample was boiled for 10 min, separated by electrophoresis on a 6% (wt/vol) polyacrylamide gel, and transferred to a nitrocellulose membrane. Nonspecific binding sites were blocked by immersing the sample in Tris-buffered saline containing 5% (wt/vol) skim milk and 0.1% Tween 20 at room temperature for 1 h. The membranes were rinsed, incubated overnight with anti–PSA-NCAM (1:1,000; Millipore) at 4 °C, and then incubated with HRP conjugate anti-goat IgG (1:2,000; Santa Cruz Biotechnology) at room temperature for 2 h. After rinsing with Tris-buffered saline containing 0.1% Tween 20, the chemiluminescence signals from the immunocomplexes were visualized by using ImageQuant LAS 4000 (GE Healthcare) according to the manufacturer's instructions. To remove sialic acids, the boiled protein samples were dried completely in a speed-vac system and redistributed in 14 μL deionized water followed by the addition of 4 μL 5× reaction buffer and 2 μL Sialidase A (Prozyme) solution containing 40 units Sialidase A. The samples were incubated at 37 °C overnight.

Instruments and Characterizations. Fluorescence and phase-contrast micrographs of neuron cultures were obtained using Olympus IX71 (Olympus) equipped with a CCD camera (DP71; Olympus). An LSM 700 META confocal microscope (Carl Zeiss) was also used to obtain the images with *Z* resolution. From the images, the lengths of major neurites were measured with the Neuron J plugin in ImageJ software (National Institutes of Health). Live-cell imaging was performed using an Olympus IX71 (Olympus) equipped with a CCD camera (iXon3; Andor). In this case, 10 mM Hepes was added to maintain the pH.

ACKNOWLEDGMENTS. This work was supported by the Basic Science Research Program through the National Research Foundation of Korea funded by Ministry of Science, ICT, and Future Planning Grants 2012R1A3A2026403 and 2012R1A2A1A01007327.

1. Wright AJ, Andrews PW (2009) Surface marker antigens in the characterization of human embryonic stem cells. *Stem Cell Res (Amst)* 3(1):3–11.
2. Varki A (2007) Glycan-based interactions involving vertebrate sialic-acid-recognizing proteins. *Nature* 446(7139):1023–1029.
3. Murrey HE, Hsieh-Wilson LC (2008) The chemical neurobiology of carbohydrates. *Chem Rev* 108(5):1708–1731.
4. Kleene R, Schachner M (2004) Glycans and neural cell interactions. *Nat Rev Neurosci* 5(3):195–208.
5. Rutishauser U (1998) Polysialic acid at the cell surface: Biophysics in service of cell interactions and tissue plasticity. *J Cell Biochem* 70(3):304–312.
6. Senkov O, Tikhobrazova O, Dityatev A (2012) PSA-NCAM: Synaptic functions mediated by its interactions with proteoglycans and glutamate receptors. *Int J Biochem Cell Biol* 44(4):591–595.
7. Vogt J, et al. (2012) Homeostatic regulation of NCAM polysialylation is critical for correct synaptic targeting. *Cell Mol Life Sci* 69(7):1179–1191.
8. Acheson A, Sunshine JL, Rutishauser U (1991) NCAM polysialic acid can regulate both cell-cell and cell-substrate interactions. *J Cell Biol* 114(1):143–153.
9. Szele FG, et al. (1994) Pattern of expression of highly polysialylated neural cell adhesion molecule in the developing and adult rat striatum. *Neuroscience* 60(1): 133–144.
10. Rutishauser U (2008) Polysialic acid in the plasticity of the developing and adult vertebrate nervous system. *Nat Rev Neurosci* 9(1):26–35.
11. Collins BE, Fralich TJ, Itonori S, Ichikawa Y, Schnaar RL (2000) Conversion of cellular sialic acid expression from *N*-acetyl- to *N*-glycolylneuraminic acid using a synthetic precursor, *N*-glycolylmannosamine pentaacetate: Inhibition of myelin-associated glycoprotein binding to neural cells. *Glycobiology* 10(1):11–20.
12. Büttner B, et al. (2002) Biochemical engineering of cell surface sialic acids stimulates axonal growth. *J Neurosci* 22(20):8869–8875.
13. Prescher JA, Bertozzi CR (2005) Chemistry in living systems. *Nat Chem Biol* 1(1):13–21.
14. Bertozzi CR, Kiessling LL (2001) Chemical glycobiology. *Science* 291(5512):2357–2364.
15. Kayser H, et al. (1992) Biosynthesis of a nonphysiological sialic acid in different rat organs, using *N*-propanoyl-D-hexosamines as precursors. *J Biol Chem* 267(24): 16934–16938.
16. Wieser JR, Heisner A, Stehling P, Oesch F, Reutter W (1996) *In vivo* modulated *N*-acyl side chain of *N*-acetylneuraminic acid modulates the cell contact-dependent inhibition of growth. *FEBS Lett* 395(2-3):170–173.
17. Keppler OT, Horstkorte R, Pawlita M, Schmidt C, Reutter W (2001) Biochemical engineering of the *N*-acyl side chain of sialic acid: Biological implications. *Glycobiology* 11(2):11R–18R.
18. Grünholz HJ, Harms E, Opetz M, Reutter W, Cerný M (1981) Inhibition of *in vitro* biosynthesis of *N*-acetylneuraminic acid by *N*-acyl- and *N*-alkyl-2-amino-2-deoxyhexoses. *Carbohydr Res* 96(2):259–270.
19. Mahal LK, Yarema KJ, Bertozzi CR (1997) Engineering chemical reactivity on cell surfaces through oligosaccharide biosynthesis. *Science* 276(5315):1125–1128.
20. Shieh P, Hangauer MJ, Bertozzi CR (2012) Fluorogenic azidofluoresceins for biological imaging. *J Am Chem Soc* 134(42):17428–17431.
21. Saxon E, Bertozzi CR (2000) Cell surface engineering by a modified Staudinger reaction. *Science* 287(5460):2007–2010.
22. Chang PV, Prescher JA, Hangauer MJ, Bertozzi CR (2007) Imaging cell surface glycans with bioorthogonal chemical reporters. *J Am Chem Soc* 129(27):8400–8401.
23. Saxon E, et al. (2002) Investigating cellular metabolism of synthetic azidosugars with the Staudinger ligation. *J Am Chem Soc* 124(50):14893–14902.
24. Prescher JA, Dube DH, Bertozzi CR (2004) Chemical remodelling of cell surfaces in living animals. *Nature* 430(7002):873–877.
25. Chang PV, et al. (2009) Metabolic labeling of sialic acids in living animals with alkynyl sugars. *Angew Chem Int Ed Engl* 48(22):4030–4033.
26. Hang HC, Yu C, Kato DL, Bertozzi CR (2003) A metabolic labeling approach toward proteomic analysis of mucin-type *O*-linked glycosylation. *Proc Natl Acad Sci USA* 100(25):14846–14851.
27. Laughlin ST, Baskin JM, Amacher SL, Bertozzi CR (2008) *In vivo* imaging of membrane-associated glycans in developing zebrafish. *Science* 320(5876):664–667.
28. de Almeida G, Sletten EM, Nakamura H, Palaniappan KK, Bertozzi CR (2012) Thiacycloalkynes for copper-free click chemistry. *Angew Chem Int Ed Engl* 51(10):2443–2447.
29. Soriano Del Amo D, et al. (2010) Biocompatible copper(I) catalysts for *in vivo* imaging of glycans. *J Am Chem Soc* 132(47):16893–16899.
30. Hsu TL, et al. (2007) Alkynyl sugar analogs for the labeling and visualization of glycoconjugates in cells. *Proc Natl Acad Sci USA* 104(8):2614–2619.
31. Dehnert KW, et al. (2011) Metabolic labeling of fucosylated glycans in developing zebrafish. *ACS Chem Biol* 6(6):547–552.
32. Rabuka D, Hubbard SC, Laughlin ST, Argade SP, Bertozzi CR (2006) A chemical reporter strategy to probe glycoprotein fucosylation. *J Am Chem Soc* 128(37): 12078–12079.
33. Dumont A, Malleron A, Awwad M, Dukan S, Vauzeilles B (2012) Click-mediated labeling of bacterial membranes through metabolic modification of the lipopolysaccharide inner core. *Angew Chem Int Ed Engl* 51(13):3143–3146.
34. Mas Pons J, et al. (2014) Identification of living Legionella pneumophila using species-specific metabolic lipopolysaccharide labeling. *Angew Chem Int Ed Engl* 53(5): 1275–1278.
35. Seki T, Arai Y (1991) The persistent expression of a highly polysialylated NCAM in the dentate gyrus of the adult rat. *Neurosci Res* 12(4):503–513.
36. Besanceney-Webler C, et al. (2011) Increasing the efficacy of bioorthogonal click reactions for bioconjugation: A comparative study. *Angew Chem Int Ed Engl* 50(35): 8051–8056.
37. Feng L, et al. (2013) Bifunctional unnatural sialic acids for dual metabolic labeling of cell-surface sialylated glycans. *J Am Chem Soc* 135(25):9244–9247.
38. Uttamapinant C, et al. (2012) Fast, cell-compatible click chemistry with copper-chelating azides for biomolecular labeling. *Angew Chem Int Ed Engl* 51(24):5852–5856.
39. Hong V, Steinmetz NF, Manchester M, Finn MG (2010) Labeling live cells by copper-catalyzed alkyne—azide click chemistry. *Bioconjug Chem* 21(10):1912–1916.
40. Du J, et al. (2009) Metabolic glycoengineering: Sialic acid and beyond. *Glycobiology* 19(12):1382–1401.
41. Charter NW, Mahal LK, Koshland DE, Jr, Bertozzi CR (2002) Differential effects of unnatural sialic acids on the polysialylation of the neural cell adhesion molecule and neuronal behavior. *J Biol Chem* 277(11):9255–9261.
42. Schmidt C, Stehling P, Schnitzer J, Reutter W, Horstkorte R (1998) Biochemical engineering of neural cell surfaces by the synthetic *N*-propanoyl-substituted neuraminic acid precursor. *J Biol Chem* 273(30):19146–19152.
43. Keppler OT, et al. (1995) Biosynthetic modulation of sialic acid-dependent virus-receptor interactions of two primate polyoma viruses. *J Biol Chem* 270(3):1308–1314.
44. Kontou M, Bauer C, Reutter W, Horstkorte R (2008) Sialic acid metabolism is involved in the regulation of gene expression during neuronal differentiation of PC12 cells. *Glycoconj J* 25(3):237–244.
45. Horstkorte R, Reinke S, Bauer C, Reutter W, Kontou M (2010) *N*-Propionylmannosamine-induced over-expression and secretion of thioredoxin leads to neurite outgrowth of PC12 cells. *Biochem Biophys Res Commun* 395(3):296–300.
46. Mahal LK, et al. (2001) A small-molecule modulator of poly-α 2,8-sialic acid expression on cultured neurons and tumor cells. *Science* 294(5541):380–381.
47. Horstkorte R, et al. (2004) Selective inhibition of polysialyltransferase ST8SiaII by unnatural sialic acids. *Exp Cell Res* 298(1):268–274.
48. Charter NW, Mahal LK, Koshland DE, Jr, Bertozzi CR (2000) Biosynthetic incorporation of unnatural sialic acids into polysialic acid on neural cells. *Glycobiology* 10(10): 1049–1056.
49. Dotti CG, Sullivan CA, Banker GA (1988) The establishment of polarity by hippocampal neurons in culture. *J Neurosci* 8(4):1454–1468.
50. Futerman AH, Banker GA (1996) The economics of neurite outgrowth—the addition of new membrane to growing axons. *Trends Neurosci* 19(4):144–149.
51. Bray D (1970) Surface movements during the growth of single explanted neurons. *Proc Natl Acad Sci USA* 65(4):905–910.
52. Seidenfaden R, Krauter A, Hildebrandt H (2006) The neural cell adhesion molecule NCAM regulates neuritogenesis by multiple mechanisms of interaction. *Neurochem Int* 49(1):1–11.
53. Nam Y, Brewer GJ, Wheeler BC (2007) Development of astroglial cells in patterned neuronal cultures. *J Biomater Sci Polym Ed* 18(8):1091–1100.
54. Ridet JL, Malhotra SK, Privat A, Gage FH (1997) Reactive astrocytes: Cellular and molecular cues to biological function. *Trends Neurosci* 20(12):570–577.
55. Ueno A, Kitawaki T, Chida N (2008) Total synthesis of (+/-)-murrayazoline. *Org Lett* 10(10):1999–2002.
56. Hennessy ET, Betley TA (2013) Complex *N*-heterocycle synthesis via iron-catalyzed, direct C-H bond amination. *Science* 340(6132):591–595.